Neuro-Oncology

25(8), 1507–1517, 2023 | https://doi.org/10.1093/neuonc/noad032 | Advance Access date 9 February 2023

Efficient detection and monitoring of pediatric brain malignancies with liquid biopsy based on patient-specific somatic mutation screening

Marija Kojic, Mellissa K. Maybury, Nicola Waddell, Lambros T. Koufariotis, Venkateswar Addala, Amanda Millar, Scott Wood, John V. Pearson, Jordan R. Hansford, Tim Hassall, and Brandon J. Wainwright

All author affiliations are listed at the end of the article

Corresponding Authors: Brandon J. Wainwright, PhD, Frazer Institute, The University of Queensland, Woolloongabba, Queensland 4102, Australia (b.wainwright@uq.edu.au); Tim Hassall, MBBS FRACP (Paed Med Onc), Children's Brain Cancer Centre, The University of Queensland, Woolloongabba, Queensland 4102, Australia (tim.hassall@health.qld.gov.au)

Abstract

Background. Brain cancer is the leading cause of cancer-related death in children. Early detection and serial monitoring are essential for better therapeutic outcomes. Liquid biopsy has recently emerged as a promising approach for detecting these tumors by screening body fluids for the presence of circulating tumor DNA (ctDNA). Here we tested the limits of liquid biopsy using patient-specific somatic mutations to detect and monitor primary and metastatic pediatric brain cancer.

Methods. Somatic mutations were identified in 3 ependymoma, 1 embryonal tumor with multilayered rosettes, 1 central nervous system neuroblastoma, and 7 medulloblastoma patients. The mutations were used as liquid biomarkers for serial assessment of cerebrospinal fluid (CSF) samples using a droplet digital PCR (ddPCR) system. The findings were correlated to the imaging data and clinical assessment to evaluate the utility of the approach for clinical translation.

Results. We developed personalized somatic mutation ddPCR assays which we show are highly specific, sensitive, and efficient in detection and monitoring of ctDNA, with a positive correlation between presence of ctDNA, disease course, and clinical outcomes in the majority of patients.

Conclusions. We demonstrate the feasibility and clinical utility of personalized mutation-based liquid biopsy for the surveillance of brain cancer in children. However, even with this specific and sensitive approach, we identified some potential false negative analyses. Overall, our results indicate that changes in ctDNA profiles over time demonstrate the great potential of our specific approach for predicting tumor progression, burden, and response to treatment.

Key Points

- Molecular profiling of pediatric brain tumors reveals a paucity of recurrent driver mutations or chromosome rearrangements.
- Screening of CSF for rare somatic mutations using personalized ddPCR assays enables sensitive and specific tumor burden surveillance.

Despite the progress of modern medicine in early diagnosis and treatment of brain cancer, it remains one of the leading causes of childhood death.[1] Tumor resection and magnetic resonance imaging (MRI) are still the primary methods for treatment, diagnosis, and postsurgical monitoring respectively. The lack of sufficient tissue sampling and the presence of nontumor tissues upon resection are common challenges for the diagnosis and classification of these tumors. Moreover, as malignant cells continuously evolve and compete with each other and the surrounding microenvironment, intratumor heterogeneity develops,[2] therefore single biopsies are not representative of the entire tumor over time. MRI often suffers from limitations in differentiating tumor-like lesions and treatment necrosis from residual disease and tumor recurrence.[3]

Importance of the Study

Significant challenges currently impose limitations on utilizing ctDNA-based liquid biopsy in the clinic for detection and surveillance of pediatric brain tumors. In this study, we characterize the ctDNA profiles of patients with medulloblastoma, ependymoma, central nervous system neuroblastoma, and embryonal tumor with multilayered rosettes, where each tumor type is shown to have a relatively stable genome and a modest frequency of driver mutations and genome rearrangements. Whilst ctDNA liquid biopsy is an attractive approach to prospectively monitor the evolution of tumor drivers, the general applicability is clearly impacted by the frequency of such drivers in the tumors. Here we present a personalized approach in ctDNA detection using whole-genome sequencing to identify rare somatic mutations and develop droplet digital PCR assays based on these mutations to screen CSF of children for the tumor DNA, to assess minimal residual disease. In a cohort of 12 patients, we show that personalized ctDNA assays are highly specific, reproducible, and sensitive, and can be efficiently used to detect down to 0.17 ng of ctDNA in 1 ml of CSF, which equates to around 50 copies of the tumor genome per ml. Moreover, we find that the method enables efficient monitoring of dynamic ctDNA changes over the course of the disease and can be used for prediction of tumor recurrence and therapy response. While our data have indicated that a ddPCR approach is highly sensitive, the clinical utility of a liquid biopsy of CSF to monitor pediatric brain tumors remains unclear. Our data and those of others suggest that a "positive" ctDNA analysis is indicative of active disease and can predict relapse ahead of imaging, albeit with a sensitivity that is currently unknown. However, the overall significance of a "negative" result is not currently evident.

Cytologic examination of CSF is routinely performed as a measure of screening for a presence of tumor cells in many cancer types. While the method is highly specific, it suffers from a lack of sensitivity (<50% confidence interval).[4] Therefore, there is an ongoing need to improve diagnostic and monitoring measures for pediatric intracranial cancers. In the light of this, liquid biopsy based on ctDNA detection is a prospective, relatively noninvasive diagnostic and monitoring approach that opens new avenues for personalized medicine for these patients.

Analysis of ctDNA from CSF has been demonstrated to be a better reflection of brain tumor somatic mutations than blood ctDNA,[5] with the dynamic changes of CSF-derived ctDNA recapitulating the disease course in patients with central nervous system (CNS) malignancies.[6–8] Liu and colleagues showed that low-coverage whole-genome sequencing (WGS) can be used to efficiently detect residual disease based on the analysis of tumor-associated copy-number changes of CSF-derived ctDNA in patients with medulloblastoma.[9] However, the tumor DNA detection rates and specificity of liquid biopsy assays show high fluctuations across different studies and thus, may not be able to meet clinical requirements,[10] especially if the method is mainly based on screening for a panel of commonly mutated genes,[11] which is a highly selective approach. Given the heterogeneous nature of brain cancer and that, compared to adult, pediatric brain tumors often have fewer somatic mutations,[12] panel-based ctDNA surveillance may be neither accurate nor reliable. Indeed, a recent study that assessed the utility of ctDNA detection using targeted panel assays across all types of brain cancer in children, found that most samples had insufficient somatic mutations to be detected, and a high rate of false-positive results was observed.[13] These challenges limit the clinical utility of ctDNA-based liquid biopsy in the majority of children with CNS malignancies.

In this study, we improve on the shortcomings of panel assay-based liquid biopsy techniques in children with brain cancer by using a highly personalized approach. We developed ddPCR assays based on patient-specific somatic mutations identified by WGS of the tumor tissue and validated their use as liquid biomarkers to detect ctDNA in longitudinally collected CSF samples of 12 children with medulloblastoma, ependymoma, CNS neuroblastoma, and embryonal tumor with multilayered rosettes (ETMR).

Materials and Methods

Patient Cohort and Sample Processing

Patient samples were obtained from a cohort of pediatric patients diagnosed with primary brain malignancies from the Queensland Children's Tumor Bank.

Freshly resected brain tumor tissue (excess to clinical requirements) was collected from the Hospital's Anatomical Pathology laboratory in sterile DMEM/F12 transport media. Tumor tissues were removed from transport media under sterile conditions within a class II biosafety cabinet, portioned into <3 mm^3 pieces in sterile 1.5 ml screw-cap tubes, snap-frozen on dry ice, then stored at –80°C prior to genomic DNA extraction.

CSF specimens were collected in 28 ml sterile universal specimen containers at the specified time points, and during standard-of-care procedures (external ventricular drain, shunt tap, or lumbar puncture). CSF specimens were temporarily stored at 4°C for up to 2 h prior to processing under sterile conditions. CSF specimens were centrifuged at 10 000 × *g* for 10 min at 4°C to separate the supernatant from cellular debris. Supernatants were aliquoted into 200–500 µl aliquots, snap-frozen on dry ice, then stored at –80°C prior to ctDNA extraction.

CSF DNA Extraction

CSF supernatants (200–500 µl) were processed for extraction of ctDNA by QIAamp Circulating Nucleic Acid Kit (Qiagen, 55114) as described by the manufacturer. The samples were eluted in 100 µl of AE buffer. The ctDNA samples were further analyzed on the Agilent Bioanalyzer 2100 system using a High Sensitivity DNA Kit (Agilent, 5067-4626). For each sample, 1 µl is loaded on the chip. Concentration and fragment size on the plots were measured in the area between 50 bp and 500 bp.

Somatic Variant Analysis

Somatic single nucleotide variants (SNVs) and indels were detected with a dual calling strategy. The consensus of two different tools was used for downstream analysis: qSNP (version 2.1.4)[14] and GATK HaplotypeCaller (version 4.0.4.0),[15] with detection of indels (1–50 bp) carried out using GATK (version 4.0.4.0). SnpEff[16] was used to perform variant annotation for gene consequence. Structural variants (SVs) were determined using qSV (https://github.com/AdamaJava/adamajava/tree/master/qsv; version 0.3).[17] SV breakpoints and potential consequences of rearrangements are annotated using ENSEMBL annotation (version 75) of known genes. Only high confidence category 1 and 2 SV calls were used in the analysis.

Pileup Approach to Determine the Presence of Somatic Mutations in ctDNA Patient Samples

A pileup approach was used to assess whether variants detected from the WGS samples were also present in the ctDNA exome sequenced sample from the same patient. Pileups were generated using the AdamaJava tool qbasepileup (https://github.com/AdamaJava/adamajava/tree/master/qbasepileup) using pileup profiles "SNV" and "DNP". The "qbasepileup" filter parameters were set with the following parameters: CIGAR_M > 34, MD_mismatch ≤ 3, Flag_DuplicateRead = false, and MAPQ > 10. The pileup approach determined the number of sequence reads at each variant genomic position across the ctDNA sequenced patient samples.

Droplet Digital PCR (ddPCR)

Somatic mutations detected from the WGS of the tumor tissue within gene coding regions were selected for ddPCR assays. Designed primers for the assays were blasted against the human genome using Primer-BLAST tool[18] to perform a specificity check.

We used QX200 droplet digital PCR (ddPCR) system (BioRad) to determine the presence of ctDNA in the CSF samples following the manufacturer's protocol. Automated Droplet Generator (BioRad, QX200, AutoDG) was used to generate approximately 20 000 droplets in a sample containing ddPCR Supermix for probes (no dUTP; BioRad, 1863024), a custom-made genotyping assay, water, and DNA sample of interest. After performing PCR amplification in a thermocycler, the plates were placed on the Droplet Reader where mutant positive (FAM), wild-type (HEX), double positive (FAM/HEX), and negative droplets were counted to provide absolute DNA quantification. The mutant and wild-type allele concentrations were determined using Quantasoft Analysis Pro software (BioRad, version 1.7) and extrapolated to copies/ml of CSF as previously described.[19]

Results

Processing and Detection of ctDNA in the CSF of Primary Pediatric Brain Tumors

We selected 12 pediatric patients diagnosed with malignant brain tumors for which there were matched diagnostic tumor tissue, peripheral blood cells, and longitudinally-collected CSF samples available in the pediatric biobank. The patients underwent tumor resection and blood and CSF collection as a part of standard-of-care clinical procedures. Collection, processing, and analysis of the samples are depicted in Figure 1A. The cohort included 7 medulloblastomas, 3 ependymomas, 1 ETMR, and 1 CNS neuroblastoma patient (Figure 1B). All patients received standard chemo- and radiotherapy where appropriate. To date, 5 patients are deceased and 7 continue in ongoing surveillance.

We collected a total of 79 liquid biopsies. For 7 patients, CSF was collected up to 1 week postsurgery and for 5 patients, we obtained these samples at later time points (Figure 1B and Supplementary Table 1). No cells were detected from the cytologic analysis in any of the samples. We used a previously established method for ctDNA extraction (refer to the Materials and Methods section) and measured DNA integrity using Bioanalyzer microchips. Electropherograms showed distinct sharp (Supplementary Figure 1A) or rounded (Supplementary Figure 1B) peaks, with a median fragment size of 175.3 bp (Supplementary Figure 1C), corresponding to ctDNA based on previous studies.[13,19,20] Sharp peaks were found in 11, rounded peaks in 15, and no peaks were detected in 48 CSF-derived samples (Supplementary Table 1). In 74 out of 79 samples, we did not detect background genomic DNA fragments (>500 bp). The method yielded a median of 45.64 ng of DNA (Supplementary Figure 1D).

Molecular Profiling of Tumors and ctDNA by NGS

We characterized the tumors at the molecular level by performing WGS to a targeted read depth of 30× for germline and 60× coverage for matching tumor DNA samples. We looked for mutations in common driver genes of respective brain tumor types and their subgroups where relevant, including but not limited to *MYCN*, *PTCH1*, *GLI2*, *CDK6*, and *SUFU* for medulloblastoma, *EZHIP*, *CDKN2A*, *NOTCH1*,[21] and *ADGRL3*[22] for ependymoma, *C19MC*, *miR-17–92*, and *DICER1* in ETMR.[23] WGS revealed that most of these genes were not mutated in the tumors (Figure 2, Supplementary Table 2 and Supplementary Table 3). Hence, commercially available ddPCR panels based on these mutations would not be useful for ctDNA screening in the CSF samples.

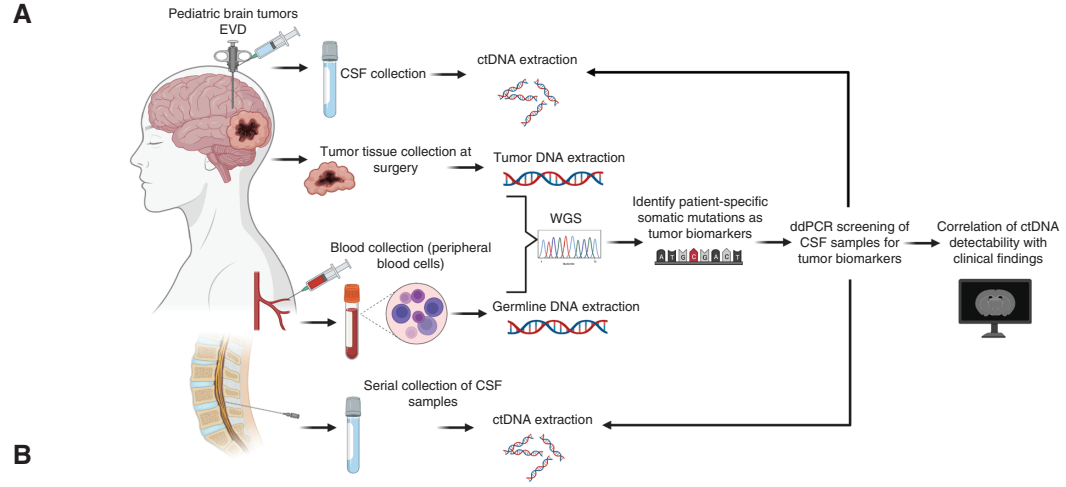

	Age*	Sex	Diagnosis*	Tumor location	Metastases*	Surgery (age)**	Surgery	Tissue pathology	Treatment	Relapse (age)	Number of CSF biopsies
Patient 1	1y 6m	♂	Ependymoma	Posterior fossa	No	0	NTR[1,2]	WHO grade II; H3K27me3 loss	RT; Chemotherapy	6y 4m†	5
Patient 2	3y 5m	♂	Ependymoma	Posterior fossa	No	0	GTR	WHO grade II; H3K27me3 loss	RT	No	10
Patient 3	11y 7m	♂	Ependymoma	Posterior fossa	No	0	GTR[1,2]; partial debulking[3]	Anaplastic; WHO grade III; 1q21 (CKS1B) duplication	Chemotherapy	13y 7m†	1
Patient 4	2y 6m	♂	ETMR	Left parietal lobe	No	0	GTR[1,4];NTR[2,3];Resection[5]	WHO grade IV; C19MC-altered	RT; Chemotherapy	3y 8m†	3
Patient 5	6y 2m	♂	Medulloblastoma	Posterior fossa	Yes	0	Near-total debulking	Mixed histology; WHO grade IV; non-WNT; non-SHH; MYCN amplification	RT; Chemotherapy	7y 4m†	6
Patient 6	10y 5m	♂	Medulloblastoma	Posterior fossa	Yes	0	GTR	Classic; WHO grade IV; non-WNT; non-SHH; MYCN amplification	RT; Chemotherapy	No	6
Patient 7	9y 9m	♀	CNS neuroblastoma	Right basal ganglia	No	1	Debulking	WHO grade III-IV; FOXR2 activation	RT; Chemotherapy	No	5
Patient 8	2y 1m	♀	Medulloblastoma	Posterior fossa	No	1	GTR	Large cell anaplastic; WHO grade IV; non-WNT; non-SHH; MYC amplification	Chemotherapy	2y 10m†	4
Patient 9	4y 3m	♂	Medulloblastoma	Posterior fossa	No	0	GTR	Classic; WHO grade IV; non-WNT; non-SHH; no MYC or NMYC amplification	RT; Chemotherapy	No	10
Patient 10	6y 9m	♀	Medulloblastoma	Posterior fossa	Yes	0	GTR	WHO grade IV; non-WNT; non-SHH	RT; Chemotherapy	No	4
Patient 11	3y 1m	♂	Medulloblastoma	Posterior fossa	Yes	4	Debulking	Large cell anaplastic; WHO grade IV; non-WNT; non-SHH; p53 wild-type	RT; Chemotherapy	No	12
Patient 12	5y 5m	♂	Medulloblastoma	Posterior fossa	Yes	0	Near-total debulking	Classic; WHO grade IV; non-WNT; non-SHH	RT; Chemotherapy	7y 8m; stable	13

Figure 1. Detection of ctDNA from serially collected CSF samples in children with primary brain tumors. (A) Study workflow. (B) Clinicopathological characteristics for the patients included in the study. Abbreviations: CNS, central nervous system; CSF, cerebrospinal fluid; ctDNA, circulating tumor DNA; ddPCR, droplet digital PCR; ETMR, embryonal tumor with multilayered rosettes; EVD, external ventricular drain; GTR, gross-total resection; m, months; NTR, near-total resection; RT, radiation therapy; WGS, whole-genome sequencing; WHO, World Health Organization; y, years,[1–5]; surgeries in order; *, at primary diagnosis; **, primary surgery (days postdiagnosis); deceased.

Using whole-exome sequencing (WES) for ctDNA analysis has the potential to enable not only tumor detection, but also monitoring tumor evolution and the emergence of subclonal heterogeneity. Although a recent study showed that assessment of CSF by WES could be used to detect glioblastoma,[24] it remains unclear whether the approach is qualified for ctDNA detection across different primary brain malignancies. To explore this, we performed WES of the CSF samples of the first five patients (Patients 1–5) collected at the earliest time point with detectable ctDNA on Bioanalyzer (Supplementary Table 1). The number of reads sequenced was high in each sample (range 117 580 492 to 242 385 372) with the percentage of mapped reads >90% for all samples (Supplementary Table 4). However, for Patients 1–4 most of the reads were PCR duplicates (95.39 to 97.20%), which means that the mean read depth for these samples was low. In contrast, the percentage of PCR duplicates for Patient 5 was lower (20.06%). Indeed, when we looked in the ctDNA WES data, we only found sequence reads supporting mutations in Patient 5 (Supplementary Table 5). The detection of somatic mutations in ctDNA of Patient 5 may be explained by a substantially higher amount of DNA in this sample (96.72 ng) relative to others (approximately 50 ng; Supplementary Table 1) which resulted in better sequence quality (less PCR duplicates).

Personalized Somatic Mutations ddPCR Assay Development and Validation

Our goal was to develop ddPCR assays based on the mutations identified in each patient to use as a robust screening method for the malignancies. Assays were designed for ten of the patients in the coding regions (missense, nonsense, and silent mutations; Table 1), with three different variants for Patients 3–5, two variants for Patients 2, 6, 7, and 9–12 and one mutation for Patient 8. A number of the somatic mutations could not be used to generate the assays given that all possible primers matched multiple regions in the genome, which would negatively affect the specificity of the assays. This meant that only one assay could be developed for Patient 8, two assays for Patient 2, and no assays for Patient 1.

To validate the performance of the ddPCR against WGS, we used the ddPCR assays to determine the mutant allele frequency (MAF) of the targeted mutations

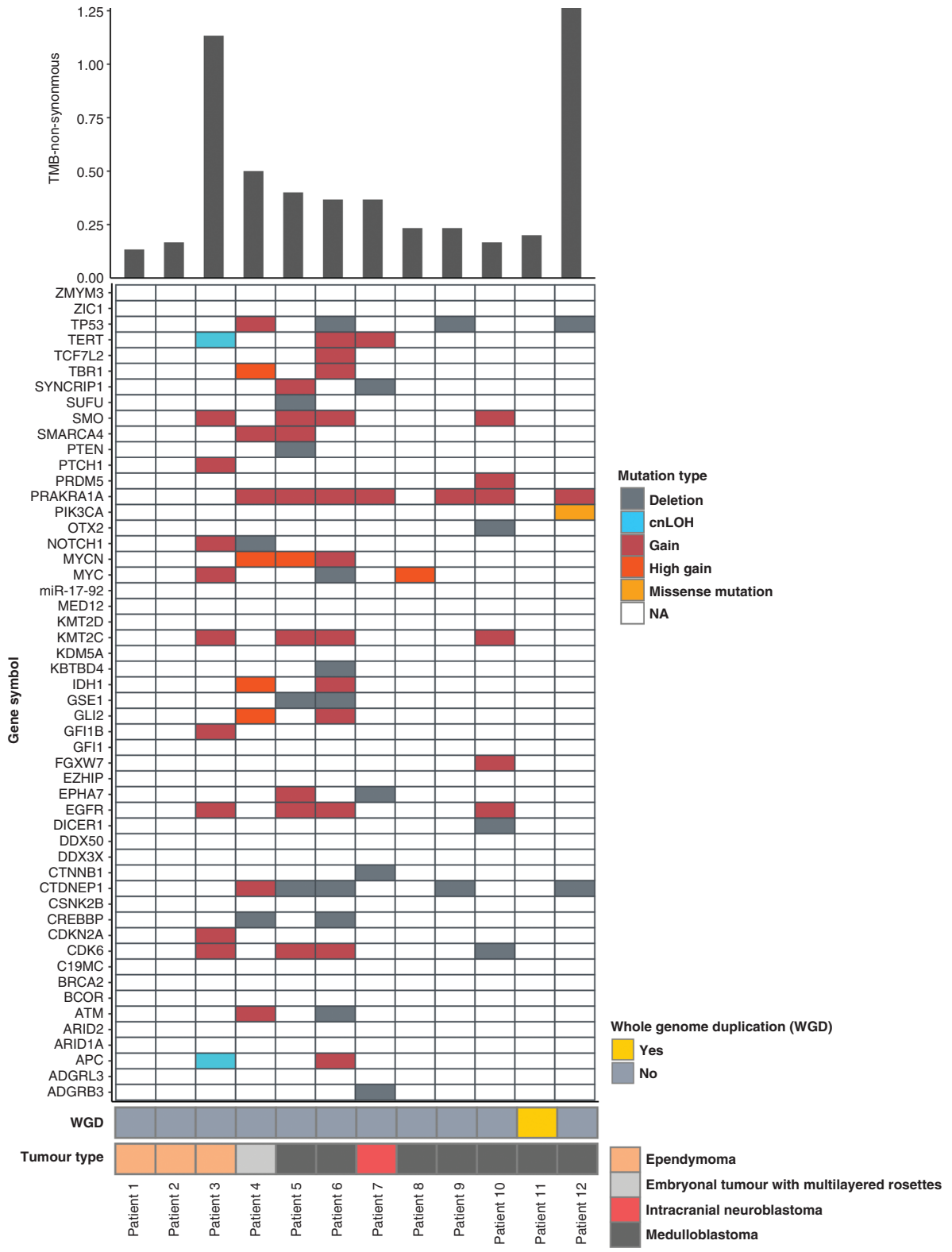

Figure 2. Molecular features of pediatric brain tumors in the study. Summary of somatic variants identified across 12 primary brain tumors (3 ependymomas, 7 medulloblastomas, 1 embryonal tumor with multilayered rosettes, and 1 CNS neuroblastoma) using whole-genome sequencing. Upper plot represents the tumor mutation burden. Mutations in selected genes are shown in the oncoplot with mutation type indicated in the color legend. The color bars below the plot show tumors with whole-genome duplication and indicate the tumor type. Abbreviations: cnLOH, copy neutral loss of heterozygosity; CNS, central nervous system; NA, not applicable; TMB, tumor mutation burden; WGD, whole-genome duplication.

Table 1. Summary of ddPCR Assays Used for ctDNA Screening

	Gene	Protein Change	MAF (WGS; %)	MAF (ddPCR; %)	LoB (Copies/Reaction)	LoD (%)
Patient 2	C1orf216	Pro134Leu	12.987	10.1987	0	1
Patient 2	ZNF318	Arg204Gln	23.6842	23.0624	0	1
Patient 3	RAD54L2	Ala304Thr	46.1538	43.567	0	1
Patient 3	POU5F2	Arg93*	84.375	86.1118	1.4396	1
Patient 3	KRT18	IleGlu275*	50	44.106	0	0.1
Patient 4	TBC1D8	Arg268Gln	45.8823	48.1692	0	1
Patient 4	CXXC1	Ala149Asp	24.359	18.1548	0	1
Patient 4	ZNF202	His583His	16.25	18.9598	1.3755	1
Patient 5	MMP14	Glu523Lys	43.2432	47.1163	0	1
Patient 5	D2HGDH	His476His	49.3671	43.9051	0	1
Patient 5	PIK3IP1	Arg140Trp	45.7627	46.7018	0	1
Patient 6	EPPK1	Arg2218His	9.7345	32.0931	1.5397	0.1
Patient 6	PTPRO	Asp975His	19.0476	19.1226	0	1
Patient 7	MROH2B	Ser586Asn	13.2075	13.324	0	1
Patient 7	NIPAL1	Ser77Asn	17.7419	13.9595	0	1
Patient 8	GPC3	Ala439Val	45.7627	44.3425	0	1
Patient 9	GMNN	Arg133His	45.4545	44.5348	0	0.1
Patient 9	SUV420H2	Arg312Leu	49.0909	42.9508	0	1
Patient 10	SLC10A5	Gln134Gln	31.25	38.8493	0	1
Patient 10	CLIP2	Gly698Arg	17.7083	20.7934	1.9397	1
Patient 11	UBR4	Thr4287Met	12.3457	10.7519	0	0.1
Patient 11	C5orf42	Arg2660*	13.3333	7.8052	1.4191	1
Patient 12	SYNP02	Leu475Gln	43.0556	33.5115	0	1
Patient 12	HNRNPR	Ala188Val	50	36.3401	0	1

Abbreviations: ctDNA, circulating tumor DNA; ddPCR, droplet digital PCR; LoB, limit of blank; LoD, limit of detection; MAF, mutant allele frequency; WGS, whole-genome sequencing; *, deletion.

(Table 1 and Figure 3A). MAF values obtained by ddPCR were highly consistent with those obtained by WGS (R^2 = 0.8684; Table 1 and Figure 3A). Bland-Altman analysis revealed relatively high levels of agreement between the two methods with the limits of agreement from –12.44% to 14.22% (Figure 3B). Thus, in the tumor tissue samples, the customized ddPCR assays exhibited comparable quantitative measurements of MAF to those identified by WGS.

To assess the specificity and sensitivity of the ddPCR assays, we quantified limit of blank (LoB) and limit of detection (LoD) of the assays respectively. The LoB across all the assays in no-template samples was between 0 and 1.9 copies/reaction (Table 1). To determine LoD, tumor DNA samples were serially diluted 10-fold in matched germline DNA, with a total of 10 ng of germline DNA used to simulate the anticipated low amount of ctDNA in the samples. LoD was quantified as the lowest fractional abundance of the mutant allele that could be statistically distinguished from that one of the neat germline samples. All ddPCR assays performed well with a good droplet separation between the mutant and wild-type allele fluorescent labels (Supplementary Figure 2) and LoD in a range from 0.1% to 1% (Table 1).

Dynamic Monitoring of ctDNA Levels in CSF Correlates with Clinical Outcomes

We explored the correlation of ctDNA concentrations in serially collected CSF samples to tumor progression and clinical outcomes. For each ddPCR assay, we loaded 14 ul of extracted ctDNA (100 ul extraction volume) of each of the samples. The number of variant copies per reaction was extrapolated to the number of variant copies per ml of CSF. The quantified ctDNA levels were compared to available clinical data and assessed on a time scale (days postdiagnosis) relative to the day of surgery and the treatment time frame.

We assessed changes in ctDNA concentrations over the course of the individual patient's disease in the cohort with a favorable clinical outcome (no relapse to date; Figures 1B and 4). In all 5 patients who had CSF samples collected at or immediately after surgery (Figure 4A–E), we were able to detect significant levels of ctDNA in the CSF. Given that none of the subsequent CSF samples were positive for ctDNA, the patients were potentially stable with no residual, and/or metastatic disease. This was in accordance with the MRI data obtained throughout and posttreatment course for all patients

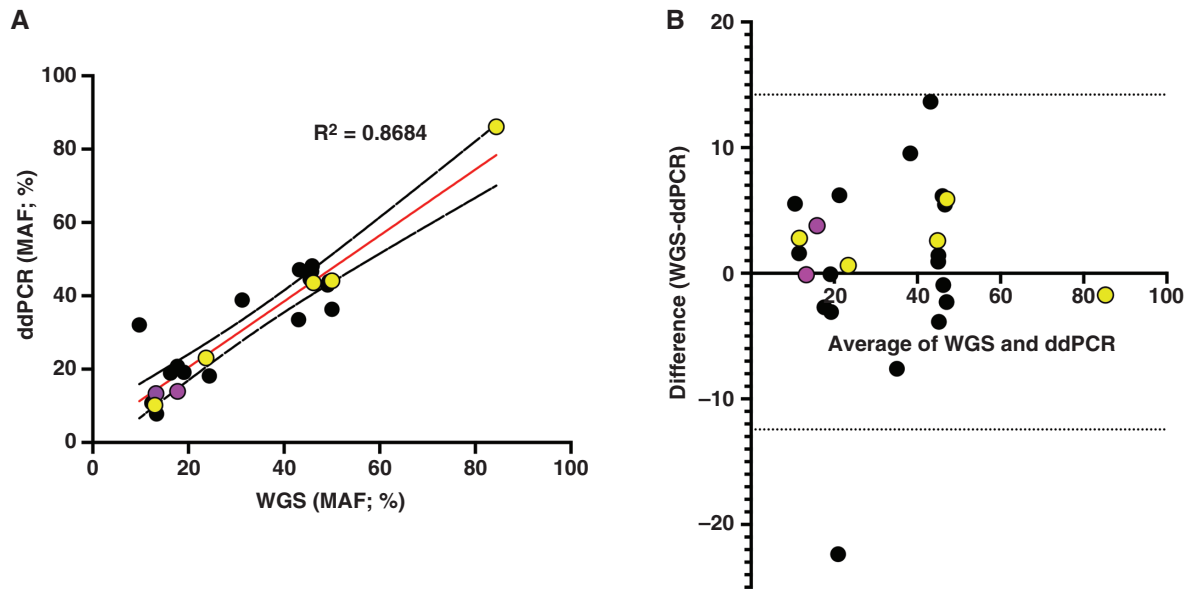

Figure 3. Comparison of mutant allele frequency in tumor tissue samples quantified from tumor tissue by WGS and ddPCR. (A) Linear regression from the comparison of WGS and ddPCR MAFs. The linear regression line is marked in red. (B) Bland-Altman plot of the differences (WGS (MAF) – ddPCR (MAF); SD of bias = 6.799). Yellow circles represent ependymoma, purple CNS neuroblastoma, and black medulloblastoma samples. For both analyses, $n = 24$. Abbreviations: CNS, central nervous system; ddPCR, droplet digital PCR; MAF, mutant allele frequency; WGS, whole-genome sequencing.

(Figure 4A–E) with the exception of Patient 12 (Figure 4E). For Patient 12, despite radiological indications of tumor relapse towards the end of the treatment course, no ctDNA was detected at any stage of treatment. Further patient monitoring will show whether this is truly a relapse or a pseudoprogression of the tumor due to the limited MRI accuracy. The first available CSF samples for Patients 10 and 2 were obtained 23 and 31 days postsurgery respectively (Figure 4F and G). Given the short half-life of ctDNA (less than 1.5 h[25]), it is not unexpected that we failed to detect the somatic mutations in these samples, especially given the successful surgical resection based on the imaging findings.

Next, we employed this method to screen for ctDNA in the cohort of patients with a poor clinical outcome (Figures 1B and 5). Although MRI imaging and clinical assessment pointed to the cancer progression in Patients 3 (ependymoma) and 4 (ETMR), we did not detect tumor DNA in their biopsies by ddPCR (Figure 5A and B). In contrast, substantial amounts of ctDNA were found across multiple CSF samples collected throughout the course of disease in two medulloblastoma patients (Patients 5 and 8) with tumor relapse confirmed by MRI (Figure 5C and D). Patient 5 (non-WNT, non-SHH MycN$^+$) underwent near-total resection and had a high amount of ctDNA at the time of surgery, and although the amount decreased postresection, the ctDNA remained detectable suggesting residual disease (Figure 5C). The levels dropped down to zero during the treatment, but progressively increased once the treatment cycle was completed. Interestingly, MRI indicated partial tumor response posttreatment with a decrease in its size whilst ctDNA analysis showed that this was a relapse, which was confirmed at the later stage by both MRI and ddPCR. Significantly high ctDNA levels were found in Patient 8 (non-WNT, non-SHH MycN$^+$) upon gross-total resection which dropped after surgery but remained detectable (Figure 5D). Residual disease was indicated after the treatment by elevated tumor DNA, whilst the imaging showed a complete remission until a later stage when the tumor mass was detected. Patients 5 and 8 were deceased at 7 years 2 months and 2 years 10 months respectively.

There was a high level of agreement between different ddPCR assays for each of the patients in following dynamic changes of ctDNA over the course of the disease (Figures 4 and 5; mean and SD values of the assays plotted for each time point). The MAF values were found to be high in the CSF samples collected close to the surgery and upon tumor relapse, resembling the MAFs of the respective tumor tissues (Table 1 and Supplementary Table 6). We were able to detect between 0.17 ng and 85.39 ng of ctDNA per 1 ml of CSF across the samples (Supplementary Table 6). The ddPCR data matched the Bioanalyzer data in most of the cases (Supplementary Table 1, Figures 4 and 5). However, Bioanalyzer analysis failed to detect ctDNA peaks for some CSF samples in Patients 5 and 8, which was not surprising due to the higher sensitivity of the ddPCR method. In several cases, we detected rounded peaks on the Bioanalyzer whilst we failed to confirm that this is tumor DNA by ddPCR. This suggests a higher confidence of sharp over rounded peaks when predicting ctDNA presence using this approach.

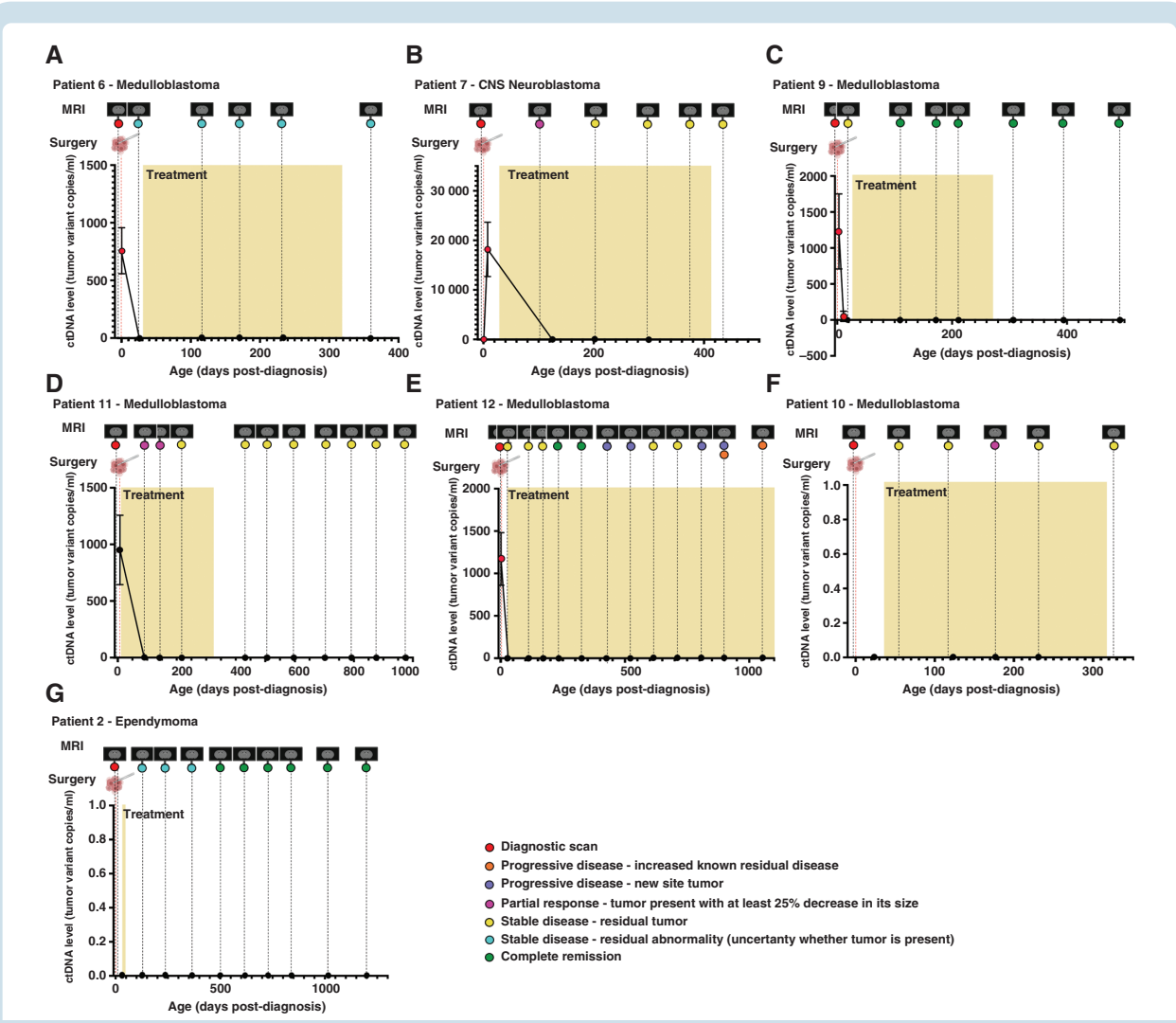

Figure 4. CSF ctDNA concentration in patients with better outcome primary pediatric brain cancer. ctDNA levels quantified by ddPCR in serially collected CSF samples are plotted against time in (A) Patient 6 (medulloblastoma), (B) Patient 7 (CNS neuroblastoma), (C–F) Patients 9–12 (medulloblastoma) and (G) Patient 2 (ependymoma). Data points in red represent ctDNA extracted from the external ventricular drain CSF samples, whilst ctDNA extracted from lumbar puncture CSF samples is marked in black. Data represent mean ± SD for the selected assays (summarized in Table 1). Surgical and imaging (MRI) time points are indicated on the plots with radiological findings provided for each time point (colors assigned as per the legend). The shaded boxes indicate treatment time frames. Abbreviations: CNS, central nervous system; CSF, cerebrospinal fluid; ctDNA, circulating tumor DNA; ddPCR, droplet digital PCR; MRI, magnetic resonance imaging.

Discussion

Due to the limitations of diagnostic tools and radiographic surveillance, detection, and monitoring of brain cancers remain challenging. Although liquid biopsy holds a great potential to address this issue, there is some variability in the claimed utility of detecting ctDNA in the CSF.[8,9,19,26–28] Recently, the largest prospective study to date of CSF-derived ctDNA across different pediatric CNS tumors discovered low sensitivity rates and false positive readings using low-coverage WGS and a targeted sequencing panel of cancer-related genes, previously shown to be highly specific and sensitive for this purpose.[13] Our study utilizes a novel approach in liquid biopsy for these tumors based on the CSF screening for patient-specific somatic mutations identified by WGS. We show that this highly personalized method is sensitive, specific, and efficient in the detection and surveillance of different brain tumor types in children, detecting as little as 0.17 ng in 1 ml of CSF. Our median ctDNA yield appeared higher in comparison to other studies,[13,29,30] and the reason for this may be that we used the Bioanalyzer for ctDNA quantification which has been shown to be a more accurate and sensitive method for DNA quantification particularly at low concentrations relative to the Qubit and TapeStation instruments,[31] which have been predominantly used for this purpose.

Most of the genetic alterations acquired by malignant cells are evolutionarily neutral.[2] Furthermore, pediatric primary brain malignancies are known to harbor fewer tumor-driver mutations relative to adult brain tumors, and other

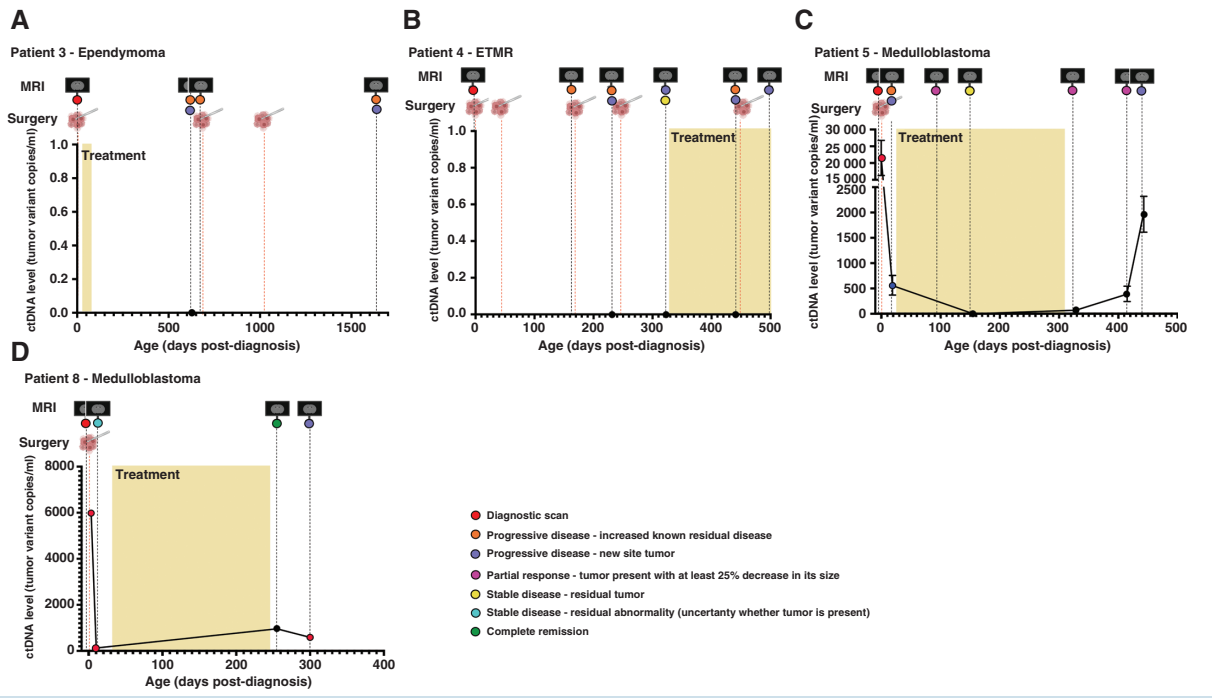

Figure 5. CSF ctDNA concentration in patients with a poor outcome primary pediatric brain cancer. ctDNA levels quantified by ddPCR in serially collected CSF samples are plotted against time in (A) Patient 3 (ependymoma), (B) Patient 4 (ETMR), (C) Patient 5 (medulloblastoma), and (D) Patient 8 (medulloblastoma). Data points in red represent ctDNA extracted from the external ventricular drain CSF samples, in blue ctDNA extracted from the shunt tap CSF, and ctDNA extracted from lumbar puncture CSF samples is marked in black. Data represent mean ± SD for the selected assays (summarized in Table 1). Surgical and imaging (MRI) time points are indicated on the plots with radiological findings provided for each time point (colors assigned as per the legend). The shaded boxes indicate treatment time frames. Abbreviations: CSF, cerebrospinal fluid; ctDNA, circulating tumor DNA; ddPCR, droplet digital PCR; MRI, magnetic resonance imaging.

types of cancer.[12] We failed to detect the most of previously reported common cancer-associated mutations in our study with WGS. We cannot fully exclude the presence of these mutations as single biopsies capture just a small part of the dynamic tumor genome. Yet, these are highly heterogeneous tumors and a one-size-fits-all approach is doomed to fail in many cases. Hence, in order to improve the performance of the surveillance routines we must shift our focus from generic sequencing panels to patient-specific mutations. These may yet be unrecognized driver or "passenger" mutations. Although cells with driver mutations are likely to be positively selected and rise in frequency, "passenger" mutations are suitable for the purpose of the tumor surveillance as long as they are somatic and subclonal (low MAF) or clonal (high MAF). Our study demonstrates that subclonal somatic mutations with MAF values as low as 7% can be used to design ddPCR assays for efficient CSF screening for ctDNA. Given that screening for a single somatic mutation may not be sufficient in some cases due to tumor evolution and clonal selection, we used at least two mutational assays in our study targeting different chromosomes. We were able to show that following only one mutation may be sufficient for monitoring these tumors as we found a high concordance of the assays for each patient. However, this is yet to be tested in a larger cohort of patients.

Tumor DNA detection in liquid biopsies can be challenging regardless of the approach taken due to a lack of ctDNA stability[25] and tumor fraction in the CSF being less than 1%.[13] Consistent with other studies, we show that ctDNA can be detected across different pediatric brain tumors and that in a number of cases its concentration likely reflects the total systemic tumor burden, as the levels decreased upon surgical resection and treatment, and increased as new lesions became apparent upon radiological examination. Thus, dynamic changes of ctDNA levels appear to reflect the state of the disease and response to treatment. We show that the high sensitivity of the ddPCR platform enables effective tumor detection even at low MAF values (<1%) when only one aliquot of CSF with a volume of less than 500 µl is used. Of note, there is a considerable amount of time required for the analysis as it takes up to 6 weeks for WGS and data analyses and 2–3 weeks to generate ddPCR probes. With the continuous advancement of technology these time frames will likely be shortened, and the platforms and analyses will become less costly, which would further improve the accessibility of the approach to the clinics worldwide.

However, despite the implementation of a highly specific and sensitive approach, we still detected a number of potential "false negative" results with MRI findings not always congruent with those of liquid biopsy throughout the course of the disease. Positive radiographic findings suspicious of active tumor burden are often found in children with no clinical recurrence. This is most likely due to the

inherent limitations of MRI in distinguishing active disease from residual lesions posttreatment. Whether these potential "false negative" results reflect the biology of the specific tumor including its location or propensity to produce ctDNA, or a technical limitation such as rapid degradation of ctDNA or the detection method itself, remains to be defined. Through the use of multiple, specific ddPCR probes on different chromosomes we have minimized the possibility of loss of overall probe binding following chromosomal rearrangements common in tumors such as medulloblastoma. Combining our data with those of previously published studies, it does appear that the presence of ctDNA is associated with relapsed disease for those tumors where we initially measured ctDNA immediately postsurgery. For example, we showed that the approach is more sensitive that the radiological surveillance given that tumor relapse was apparent by liquid biopsy analysis in two patients at an earlier stage than by using MRI.

Of note, we found that WES analyses could be performed on ctDNA studies. A recent study performed WES to analyze ctDNA in the CSF of 4 medulloblastoma patients and successfully generated libraries with an input of 6–200 ng of ctDNA.[8] In our hands, high quality libraries could be generated with ctDNA amounts over 100 ng but we were not successful using 50 ng or less of starting material. For some patients, a combination of ddPCR and WES may provide a detailed characterization of the molecular changes in response to therapy and tumor evolution. It is also of significant interest that de novo methylomes can be generated from relatively low amounts of CSF-derived ctDNA,[32] and that methylome studies per se have proved to be highly instructive in a number of different pediatric tumor types.[33–35] Due to the limited amounts of samples left following WGS and ddPCR analyses, we were not able to test the clinical application of ctDNA methylation assays in our study. Utilizing WES and methylome analysis approaches may fully remove the need for tumor tissue profiling in the future for the patients with sufficient amounts of CSF-derived ctDNA.

Overall, while our data have indicated that a ddPCR approach is highly sensitive, the clinical utility of a liquid biopsy of CSF to monitor pediatric brain tumors remains unclear. Our data and those of others suggest that a "positive" ctDNA analysis is indicative of active disease and can predict relapse ahead of imaging albeit with a sensitivity that is currently unknown. However, the overall significance of a "negative" result is not evident and awaits the collection and analysis of large numbers of patients and samples through international consortia. Given the reported short half-life of ctDNA, it also remains to be determined whether a robust liquid biopsy approach will be critically dependent on highly streamlined sample ascertainment where the CSF needs to be processed at the point of collection, for example.

We suggest that the ddPCR approach described here could form the backbone of a standard approach to liquid biopsy of CSF. A gene-specific panel, low-cover WGS, or WES could also be added on a patient-specific basis to study tumor evolution in more detail, depending upon the amount of ctDNA available and the clinical question being addressed.

Supplementary Material

Supplementary material is available online at *Neuro-Oncology* (http://neuro-oncology.oxfordjournals.org/).

Keywords:

CSF | ctDNA | liquid biopsy | pediatric brain cancer | somatic mutations

Funding

This work was supported by the Children's Hospital Foundation. N.W. is supported by an Australian National Health and Medical Research Council fellowship (1139071).

Acknowledgments

The authors are grateful to the patients who participated in this study. Figure 1A was created with BioRender.com.

Conflict of interest statement. N.W. and J.V.P. are co-founders of genomiQa and members of its Board. All other authors declare that they have no conflict of interest.

Authorship statement. B.J.W., T.H. and J.R.H. designed and directed the study. Patient recruitment, collection of the clinical samples and clinical data was performed by M.K.M. and T.H. M.K. extracted all germline and tumor DNA samples. M.K. and A.M. extracted ctDNA from CSF samples and performed ddPCR analysis. WGS and WES was performed by the Australian Genome Research Facility Ltd. N.W., R.K. and V.A. performed analysis and interpretation of sequence data. S.W. and J.V.P. were responsible for data management and software development. M.K. designed ddPCR assays, analyzed ddPCR data and made the figures and tables. The manuscript was written by M.K. and revised by B.J.W. with all authors discussing the results, providing feedback and approving the final version of it.

Affiliations

Frazer Institute, The University of Queensland, Woolloongabba, Queensland 4102, Australia (M.K., A.M., B.J.W.); Queensland Children's Tumor Bank, The University of Queensland, Child Health Research Centre, South Brisbane, Queensland 4101, Australia (M.K.M.); Children's Brain Cancer Centre, The University of Queensland, Woolloongabba, Queensland 4102, Australia (M.K.M., T.M., B.J.W.); Medical Genomics, QIMR

Berghofer Medical Research Institute, Brisbane, Queensland 4006, Australia (N.W., L.T.K., V.A., S.W., J.V.P.); Children's Cancer Centre, Royal Children's Hospital, Murdoch Children's Research Institute, University of Melbourne, Melbourne, Australia (J.R.H.); Michael Rice Cancer Centre, Women's and Children's Hospital, South Australia Health and Medical Research Institute, Adelaide, Australia (J.R.H.); Oncology Service, Queensland Children's Hospital, Children's Health Queensland Hospital and Health Service, Brisbane, Queensland 4101, Australia (T.M.)

References

1. Steliarova-Foucher E, Colombet M, Ries LAG, et al; IICC-3 contributors. International incidence of childhood cancer, 2001-10: a population-based registry study. *Lancet Oncol*. 2017; 18(6):719–731.
2. Merlo LMF, Pepper JW, Reid BJ, Maley CC. Cancer as an evolutionary and ecological process. *Nat Rev Cancer*. 2006; 6(12):924–935.
3. Verma N, Cowperthwaite MC, Burnett MG, Markey MK. Differentiating tumor recurrence from treatment necrosis: a review of neuro-oncologic imaging strategies. *Neuro-oncology*. 2013; 15(5):515–534.
4. Chamberlain MC, Glantz M, Groves MD, Wilson WH. Diagnostic tools for neoplastic meningitis: detecting disease, identifying patient risk, and determining benefit of treatment. *Semin Oncol*. 2009; 36(4 Suppl 2):S35–S45.
5. De Mattos-Arruda L, Mayor R, Ng CKY, et al. Cerebrospinal fluid-derived circulating tumour DNA better represents the genomic alterations of brain tumours than plasma. *Nat Commun*. 2015; 6(1):8839.
6. Bobillo S, Crespo M, Escudero L, et al. Cell free circulating tumor DNA in cerebrospinal fluid detects and monitors central nervous system involvement of B-cell lymphomas. *Haematologica*. 2021; 106(2):513–521.
7. Miller AM, Shah RH, Pentsova EI, et al. Tracking tumour evolution in glioma through liquid biopsies of cerebrospinal fluid. *Nature*. 2019; 565(7741):654–658.
8. Escudero L, Llort A, Arias A, et al. Circulating tumour DNA from the cerebrospinal fluid allows the characterisation and monitoring of medulloblastoma. *Nat Commun*. 2020; 11(1):5376.
9. Liu APY, Smith KS, Kumar R, et al. Serial assessment of measurable residual disease in medulloblastoma liquid biopsies. *Cancer Cell*. 2021; 39(11):1519–1530.e4.
10. Saenz-Antoñanzas A, Auzmendi-Iriarte J, Carrasco-Garcia E, et al. Liquid biopsy in glioblastoma: opportunities, applications and challenges. *Cancers (Basel)*. 2019; 11(7):950.
11. Abou Daya S, Mahfouz R. Circulating tumor DNA, liquid biopsy, and next generation sequencing: a comprehensive technical and clinical applications review. *Meta Gene*. 2018; 17:192–201.
12. Ramkissoon SH, Bandopadhayay P, Hwang J, et al. Clinical targeted exome-based sequencing in combination with genome-wide copy number profiling: precision medicine analysis of 203 pediatric brain tumors. *Neuro-oncology*. 2017; 19(7):986–996.
13. Pagès M, Rotem D, Gydush G, et al. Liquid biopsy detection of genomic alterations in pediatric brain tumors from cell-free DNA in peripheral blood, CSF, and urine. *Neuro-Oncology*. 2022; 24(8):1352–1363.
14. Kassahn KS, Holmes O, Nones K, et al. Somatic point mutation calling in low cellularity tumors. *PLoS One*. 2013; 8(11):e74380e74380.
15. McKenna A, Hanna M, Banks E, et al. The Genome Analysis Toolkit: a MapReduce framework for analyzing next-generation DNA sequencing data. *Genome Res*. 2010; 20(9):1297–1303.
16. Cingolani P, Platts A, Wang LL, et al. A program for annotating and predicting the effects of single nucleotide polymorphisms, SnpEff: SNPs in the genome of Drosophila melanogaster strain w1118; iso-2; iso-3. *Fly*. 2012; 6(2):80–92.
17. Hayward NK, Wilmott JS, Waddell N, et al. Whole-genome landscapes of major melanoma subtypes. *Nature*. 2017; 545(7653):175–180.
18. Ye J, Coulouris G, Zaretskaya I, et al. Primer-BLAST: A tool to design target-specific primers for polymerase chain reaction. *BMC Bioinf*. 2012; 13(1):134.
19. Izquierdo E, Proszek P, Pericoli G, et al. Droplet digital PCR-based detection of circulating tumor DNA from pediatric high grade and diffuse midline glioma patients. *Neurooncol Adv*. 2021; 3(1):vdab013.
20. Underhill HR, Kitzman JO, Hellwig S, et al. Fragment length of circulating tumor DNA. *PLoS Genet*. 2016; 12(7):e1006162.
21. Yao Y, Mack SC, Taylor MD. Molecular genetics of ependymoma. *Chin J Cancer*. 2011; 30(10):669–681.
22. Wang J, S-y X, Zhao Q, et al. Driver mutations in ADGRL3 are involved in the evolution of ependymoma. *Lab Investig*. 2022; 102(7):702–710.
23. Lambo S, Gröbner SN, Rausch T, et al. The molecular landscape of ETMR at diagnosis and relapse. *Nature*. 2019; 576(7786):274–280.
24. Duan H, Hu JL, Chen ZH, et al. Assessment of circulating tumor DNA in cerebrospinal fluid by whole exome sequencing to detect genomic alterations of glioblastoma. *Chin Med J (Engl)*. 2020; 133(12):1415–1421.
25. Diehl F, Schmidt K, Choti MA, et al. Circulating mutant DNA to assess tumor dynamics. *Nat Med*. 2008; 14(9):985–990.
26. Martínez-Ricarte F, Mayor R, Martínez-Sáez E, et al. Molecular diagnosis of diffuse gliomas through sequencing of cell-free circulating tumor DNA from cerebrospinal fluid. *Clin Cancer Res*. 2018; 24(12):2812–2819.
27. Wang Y, Springer S, Zhang M, et al. Detection of tumor-derived DNA in cerebrospinal fluid of patients with primary tumors of the brain and spinal cord. *Proc Natl Acad Sci U S A*. 2015; 112(31):9704–9709.
28. Huang TY, Piunti A, Lulla RR, et al. Detection of Histone H3 mutations in cerebrospinal fluid-derived tumor DNA from children with diffuse midline glioma. *Acta Neuropathol Commun*. 2017; 5(1):28.
29. Fitzpatrick A, Iravani M, Mills A, et al. Assessing CSF ctDNA to improve diagnostic accuracy and therapeutic monitoring in breast cancer leptomeningeal metastasis. *Clin Cancer Res*. 2022; 28(6):1180–1191.
30. Shah M, Takayasu T, Zorofchian Moghadamtousi S, et al. Evaluation of the Oncomine Pan-Cancer Cell-Free assay for analyzing circulating tumor dna in the cerebrospinal fluid in patients with central nervous system malignancies. *J Mol Diagn*. 2021; 23(2):171–180.
31. Hussing C, Kampmann M, Mogensen H, Børsting C, Morling N. Comparison of techniques for quantification of next-generation sequencing libraries. *Forensic Sci Int Genet Suppl Ser*. 2015; 5:e276–e278.
32. Ye Z, Chatterton Z, Pflueger J, et al. Cerebrospinal fluid liquid biopsy for detecting somatic mosaicism in brain. *Brain Commun*. 2021; 3(1):fcaa235.
33. Li J, Zhao S, Lee M, et al. Reliable tumor detection by whole-genome methylation sequencing of cell-free DNA in cerebrospinal fluid of pediatric medulloblastoma. *Sci Adv*. 2020; 6(42):eabb5427.
34. Hovestadt V, Jones DTW, Picelli S, et al. Decoding the regulatory landscape of medulloblastoma using DNA methylation sequencing. *Nature*. 2014; 510(7506):537–541.
35. Capper D, Jones DTW, Sill M, et al. DNA methylation-based classification of central nervous system tumours. *Nature*. 2018; 555(7697):469–474.